*Graphical Abstract (for review)

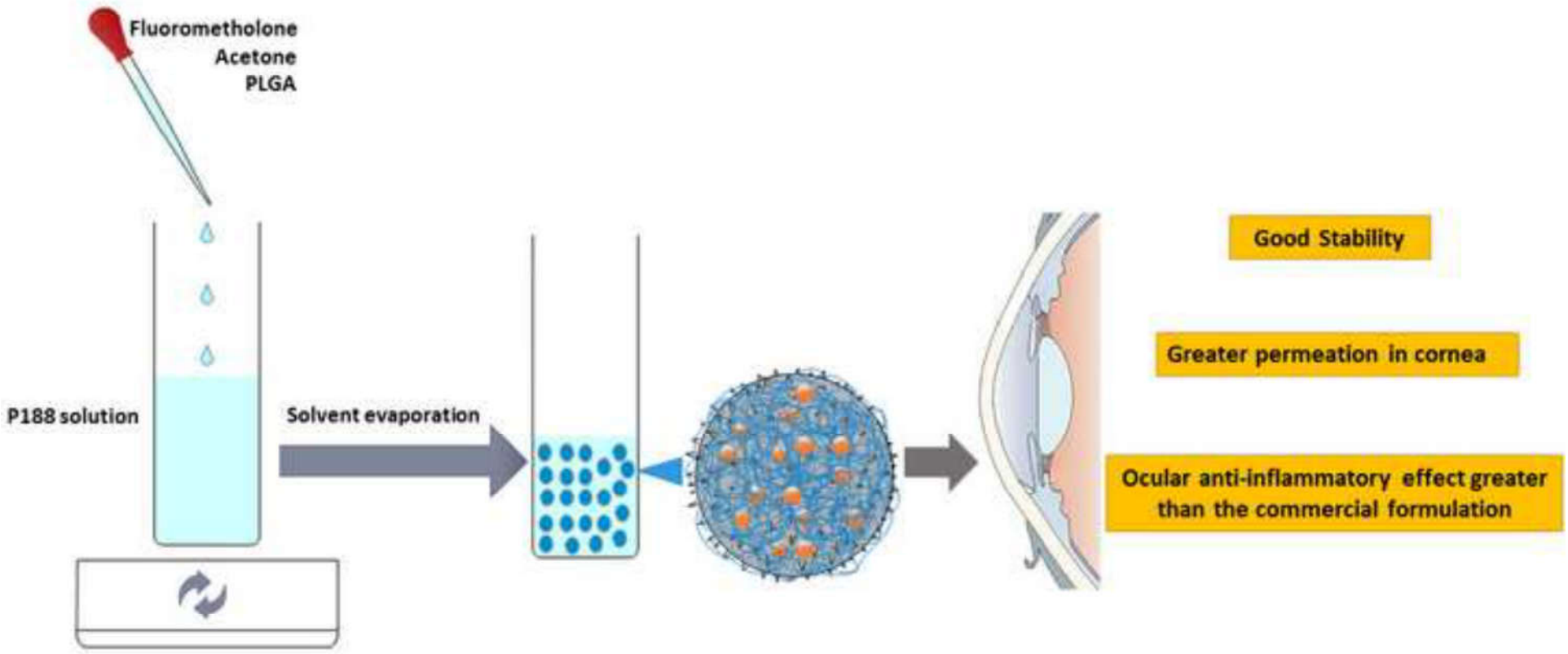

TITLE

Development of Fluorometholone-loaded PLGA Nanoparticles for Treatment of Inflammatory Disorders of Anterior and Posterior Segments of the Eye

Roberto Gonzalez-Pizarro[a,b], Marcelle Silva-Abreu[a,b], Ana Cristina Calpena[a,b], María Antonia Egea[a,b], Marta Espina[a,b], María Luisa García[a,b].

[a]Department of Pharmacy, Pharmaceutical Technology and Physical Chemistry, Faculty of Pharmacy and Food Sciences, University of Barcelona, 08028 Barcelona, Spain.

[b]Institute of Nanoscience and Nanotechnology (IN2UB), University of Barcelona, Barcelona, Spain.

ABSTRACT

The main objective of this study was the development and optimization of Fluorometholone-loaded PLGA nanoparticles for the treatment of inflammatory conditions of the eye. Design of experiments was used to obtain nanoparticles with the best physicochemical characteristics. The optimized nanoparticles containing 1.5 $mg \cdot mL^{-1}$ of Fluorometholone showed a negative surface charge (-30 mV) and an average size below 200 nm being suitable for ocular administration. Drug-polymer interaction studies confirmed no new bonds were formed during the synthesis. Nanoparticles performance was assessed with biopharmaceutical behavior studies, ocular tolerance, anti-inflammatory efficacy and bioavailability. The biopharmaceutical behavior of the drug from nanoparticles was adjusted to hyperbola order showing a significantly greater permeation in the cornea than in the sclera. The optimized formulation had significantly greater anti-inflammatory effects than the commercial formulation. In addition, nanoparticles increased drug penetration toward the vitreous. Polymeric nanoparticles of Fluorometholone could provide a suitable alternative for the treatment of inflammatory disorders of the anterior and posterior segments of the eye against of conventional topical formulations.

KEY WORDS

Fluorometholone; nanoparticles; permeation; ocular anti-inflammatory; PLGA; drug delivery.

1. Introduction

The treatment of inflammatory eye diseases such as severe allergic conjunctivitis and uveitis is focused on the use of corticosteroids as anti-inflammatory drugs (Bielory et al., 2010). These ophthalmic drugs used topically have certain disadvantages ranging from the low amount of drug penetrating through the cornea to the limited residence time in the precorneal area. This causes that the suspensions need to be administered a greater many times per day to obtain a significant therapeutic effect (Gause et al., 2016). In other cases, in which the posterior segment is affected, as in posterior uveitis, intravitreal injections are used so that the drug can reach the target (Yasin et al., 2014). Moreover, the main ocular side effect after topical administration of corticosteroids include cataracts and increased intraocular pressure, which could induce visual disorders. Among all the corticosteroids, Fluorometholone (FMT) is characterized by a highest pharmacological potency for inflammations of the anterior segment of the eye with a significantly lower risk of increasing intraocular pressure (Chen et al., 2016; Shokoohi-Rad et al., 2017).

Currently, the encapsulation of drugs in polymer matrices has been one of the solutions for overcoming the disadvantages presented by ophthalmic suspensions (Danhier et al., 2012). Particularly, PLGA nanoparticles (NPs) have proven to be one of the most suitable topical ocular administration systems, due to their sustained and prolonged release of the drug, mainly produced by diffusion (Kapoor et al., 2015). Once the NPs have been administered, the PLGA hydrolyzes in monomers (lactic acid and glycolic acid) with subsequent metabolism in the Krebs cycle, which makes this polymer highly biodegradable and biocompatible (Anderson and Shive, 2012; Diebold and Calonge, 2010; Makadia and Siegel, 2011).

In other studies, it has been shown that PLGA NPs are able to cross the tear film and the cornea, with the possibility of reaching deeper tissues such as the vitreous and the retina (Silva-Abreu et al., 2018; Tahara et al., 2017). In different reports, PLGA has been shown to

protect the drug from deactivation by the enzyme cytochrome P450 present in the tear film, corneal epithelium and ciliary, increasing the half-life of the drug (Guengerich, 2017). According to the above, these systems would allow to reduce the side effects associated with the drug with a sustained and safe release without the need for repeated administrations (Siddique et al., 2015).

The main objective of this study was the development of FMT loaded-PLGA NPs (FMT-PLGA-NPs) able to reach tissues of the anterior and posterior segment of the eye with the aim to be administered less often than medications currently marketed. The physicochemical properties, drug-polymer interaction, short-term stability and *in vitro*/*ex vivo* biopharmaceutical behavior were also assayed. Ocular tolerance, *in vivo* anti-inflammatory efficacy and ocular bioavailability of FMT-PLGA-NPs were carried out as evidence of effectivity and usefulness of NPs as a novel treatment for ocular inflammatory disorders.

2. Material and methods

2.1. Materials

FMT was purchased from Capot Chemical (Hangzhou, China). PLGA RG 503H was obtained from Evonik Corporation (Birmingham, USA). Poloxamer 188 (P188) and Transcutol® were given from BASF (Barcelona, Spain) and Gattefossé (Madrid, Spain), respectively. Acetone was purchased from Fisher Scientific (Pittsburgh, USA). Water through Millipore® MilliQ system was used for all the experiments and all the other reagents were of analytical grade.

2.2. Preparation and optimization of NPs

FMT-loaded PLGA NPs were prepared by solvent displacement method described elsewhere (Cañadas et al., 2016; Fessi et al., 1989). Briefly, PLGA (5.6–12.4 $mg \cdot mL^{-1}$) and the FMT (0.16–1.84 $mg \cdot mL^{-1}$) were dissolved in 5 mL of acetone. This organic phase was added slowly dropwise, under moderate stirring, into 10 mL of an aqueous solution of P188 (1.6–18.4 $mg \cdot mL^{-1}$) adjusted to pH 7.4. The NPs resulting were stirred for 10 min. After that, acetone was evaporated under reduced pressure.

Design of experiments (DoE) was employed using central composite design matrix generated by StatGraphics Centurion XV. The central composite design was developed to analyze the effects of the independents variables on the dependents (Nekkanti et al., 2015). Three factors (concentration of surfactant [cP188], drug [cFMT] and polymer [cPLGA]), 3-level central composite design on the measured response (average particle size (Zav), polydispersity index (PI), zeta potential (ZP) and entrapment efficiency (EE)) were established for this optimization procedure. Each factor was studied at five different levels coded (see Table I) and the responses were modelled through the full second-order polynomial equation:

$$Y = \beta_0 + \beta_1 X_1 + \beta_2 X_2 + \beta_3 X_3 + \beta_{11} X_1^2 + \beta_{22} X_2^2 + \beta_{33} X_3^2 + \beta_{12} X_1 X_2 + \beta_{13} X_1 X_3 + \beta_{23} X_2 X_3 \quad (1)$$

where Y is the measured response, β_0 to β_{23} are the regression coefficients and X_1, X_2 and X_3 are the studied factors (Cano et al., 2018).

Table I: Variables and codes used in the experimental design.

Factor (mg·mL^{-1})	Levels				
	-1.68	-1	0	+1	+1.68
cFMT	0.16	0.50	1.00	1.50	1.84
cPLGA	5.60	7.00	9.00	11.00	12.40
cP188	1.60	5.00	10.00	15.00	18.40

2.3. Analysis of NPs

Zav, PI, and ZP of NPs were determined by dynamic light scattering (DLS) and electrophoretic mobility, respectively, in a Zetasizer NanoZS (Malvern Instruments, Malvern, UK). Samples were diluted (1:10) and the experiments were performed with disposable capillary cells DTS1070 (Malvern Instruments) at 25 °C. The reported values correspond to the mean ± SD of three different batches of each NPs formulation.

The morphological examination of the NPs formulations was carried out by Transmission Electron Microscopy (TEM) on a Jeol model 1010. To visualize the NPs, copper grids carbon-coated (carbon only) were activated with a glow discharge vacuum system. Samples (10 µL) were placed on grids and negative staining performed with 2 % uranyl acetate.

The EE of FMT in the NPs was quantified indirectly by measuring the non-entrapped drug in the dispersion medium. The free FMT was separated by a filtration/centrifugation technique (1:10 dilution) by using an Amicon Ultracell–100 kDa (Amicon® Ultra; Millipore Corporation, Massachusetts, USA) centrifugal filter devices at 25 °C and 5000 rpm for 10 min (Heraeus, Multifuge 3 L-R, Centrifuge. Osterode, GER). The EE was calculated according to the following equation:

$$\mathrm{EE}\ (\%) = \frac{cFMT_0 - cFMT_1}{cFMT_0} \cdot 100 \qquad (2)$$

where $cFMT_0$ and $cFMT_1$ are the total amount of FMT and free FMT in the supernatant, respectively. The samples were evaluated by a modified pharmacopeia method of RP-HPLC and validated according to the guidelines of the International Conference on Harmonization (ICH, 2005; USP 29-NF 24, 2006). Briefly, samples were quantified using HPLC Waters 2695 separation module and a Kromasil® C18 column (5 µm, 150 × 4.6 mm) with a mobile phase of methanol/water (65:35) at a flow rate of 1.0 mL·min^{-1}. A diode array detector Waters® 2996 at a wavelength of 239 nm was used to detect the FMT. A volume of 10 µL of sample was injected. Data were processed using Empower 3® Software.

2.4. Interaction studies

2.4.1. X-ray diffraction (XRD) analysis

The state amorphous or crystalline of the drug in the NPs were determined by x-ray spectral measurements using Siemens D500 system (Karlsruher, GER). X-ray powder diffractograms were recorded using a Cu K” radiation (45 kV, 40 mA, λ= 1.544 Å) in the range (2θ) from 2° to 60° with a step size of 0.026° and measuring time of 195.8 s per step.

2.4.2. Fourier transform infrared (FTIR) analysis

FTIR spectra of NPs and compounds separately were obtained using a Thermo Scientific Nicolet iZ10 with an ATR diamond and DTGS detector. The scanning range was 525–4000 cm^{-1}.

2.4.3. Differential scanning calorimetry (DSC) analysis

Thermograms were obtained on a Mettler TA 4000 system (Greifensee, Switzerland) equipped with a DSC 25 cell. The temperature was calibrated by the melting transition point of indium prior to sample analysis. All samples were weighed (Mettler M3 Microbalance) directly in perforated aluminum pans (approximate weight of 2.5 mg), heated (under a nitrogen flow) at a rate of 2 °C·min^{-1} from 20 °C to 120 °C together to an empty pan used as a reference. Data were evaluated using the Mettler STARe V 9.01 DB software (Mettler-Toledo).

2.5. Biopharmaceutical behavior

2.5.1. *In vitro* release study

To identify the release profile of the FMT from the polymer matrix of NPs, a study was carried out in amber Franz cells (15 mm diameter). A dialysis membrane MW 12000–14000 Da (Iberoamerica, Spain) was hydrated with the receptor medium methanol/water (65:35) for 24 h before mounted. The FMT-PLGA-NPs were compared with a commercial eye drops (Isoptoflucon® of 1 mg·mL^{-1}) and the free drug (1 mg·mL^{-1}) dissolved in phosphate buffer solution at pH 7.4. The sink conditions were sustained throughout the experiment for 46 h (Klose et al., 2011). A volume of 300 µL of the samples was placed in the donor compartment and the receptor compartment was filled with receptor medium thermoregulated at 37° ± 0.5 °C in continuous agitation. Samples of 300 µL were withdrawn from the receptor compartment at fixed times and replaced by an equal volume of fresh receptor medium at the same temperature. The concentration of FMT released was measured by RP-HPLC. Values are reported as the mean ± SD of the triplicates. Akaike's information criterion (AIC) and coefficient correlation (r^2) were determined for each model as an indicator of the model's suitability (Ramos Yacasi et al., 2016).

2.5.2. *Ex vivo* corneal and sclera permeation study

The *ex vivo* FMT permeation from FMT-PLGA-NPs was evaluated using isolated pig cornea and sclera using Franz cells (9 mm diameter). Pig eyes (Landrace and Large White hybrid weighing 45–60 kg) were supplied from the Faculty of Medicine at Barcelona University, Spain. All

experiments were developed following the Association for Research in Vision and Ophthalmology on the Use of Animals in Ophthalmic and Vision Research guidelines. These were approved by the Ethical Committee of the University of Barcelona (number 7428) and the Committee of Animal Experimentation of the Regional Autonomous Government of Catalonia, Spain (Law 32/2007 of November 7, 2007, and "Real Decreto 1201/2005", October 10, 2005). The pigs were sedated by intramuscular administration of ketamine (3 $mg \cdot kg^{-1}$), xylazine (2.5 $mg \cdot kg^{-1}$) and midazolam (0.17 $mg \cdot kg^{-1}$) and euthanized by an overdose of sodium thiopental (100 $mg \cdot kg^{-1}$) under deep propofol anesthesia (1 $mg \cdot kg^{-1}$). Eyes were removed and immediately excised. The cornea and sclera were fixed in Franz cells with a diffusion segment of 0.64 cm^2. In all, 200 µL of the test formulation (FMT-PLGA-NPs and Isoptoflucon® of 1 $mg \cdot mL^{-1}$) were incubated in Franz cells and filled with Transcutol®P/water (65:35). In all experiments, a constant temperature, thermoregulated with a water jacket of 32° ± 0.5 °C and 37° ± 0.5 °C was used for the cornea and sclera, respectively, with agitation at 600 rpm. Samples of 300 µL were withdrawn from the receptor compartment at fixed times and replaced by an equal volume of fresh receptor medium at the same temperature. Sink conditions were maintained throughout the experiment.

To quantify the retained amount of drug (Q_R) in the tissues tested, at the end of the permeation study, tissues were removed from each Franz cell. The cornea and sclera were cleaned using a 0.05 % solution of sodium lauryl sulfate and washed with water. Afterward, the permeation segment of the tissues was excised, weighed and treated with methanol/water (65:35) under sonication for 15 min. FMT concentration was quantified using Triple Quadrupole LC/MS/MS Mass Spectrometer (Perkin-Elmer AB Sciex Instruments) in MRM (multiple reaction monitoring). The separate module was HPLC Agilent 1200 series equipped with an atmospheric pressure electrospray ionization ion source. The separation of the drug was carried out on reverse phase column (Kromasil® C18 of 5 µm, 150 × 4.6 mm) using a mobile phase composed of methanol/0.1% formic acid in water (65:35) at a flow rate of 0.6

$mL \cdot min^{-1}$. Mass variation was recorded at 321.4 and 279.2 Da. Values were reported as the mean ± SD. All the experiments were performed by triplicate.

Permeation parameters were calculated by plotting the cumulative FMT permeating versus time, determining x-intercept by linear regression analysis. The permeability coefficient (K_P) ($cm \cdot h^{-1}$), steady-state flux (J) ($ng \cdot h^{-1} \cdot cm^{-2}$) and amount of permeated at 24 h (Q_{24}) (µg) were calculated (Carvajal-Vidal et al., 2017).

2.6. Stability analysis of NPs

The physical stability of the NPs at 4 °C and 25 °C were evaluated by Static Multiple Light Scattering technology (S-MLS) using Turbiscan® Lab. S-MLS identifies the different destabilization phenomena of the colloidal suspension such as creaming, sedimentation, flocculation, and coalescence. NPs were placed in a cylindrical glass measuring cell that was scanned by a pulsed near-infrared light source (λ= 880 nm) with two synchronous optical detectors (transmission and backscattering). Due to the opacity of the NPs formulation, only the backscattering profiles were used to evaluate the physical stability. The backscattering data were recorded every 24 h at different times after preparation (1, 15 and 30 days).

2.7. Ocular tolerance

2.7.1. *In vitro* ocular tolerance

In vitro ocular tolerance was assessed using the HET-CAM® test in order to ensure that the formulation of FMT-PLGA-NPs are not irritating when they are administered as eye-drops. Irritation, coagulation and hemorrhage phenomena were measured by applying 300 µL of the formulation studied on chorioallantoic membrane of a fertilized chicken egg, monitoring it during the first 5 min after the application. This assay was conducted according to the guidelines of ICCVAM (The Interagency Coordinating Committee on the Validation of Alternative Methods). The development of the test was carried out with 6 eggs for each formulation (FMT-PLGA-NPs and Isoptoflucon®), 3 for controls positive (NaOH 0.1 M) and

negative (0.9 % NaCl). The ocular irritation index (OII) was calculated by the sum of the scores of each injury according to the following expression:

$$OII = \frac{(301-h)\cdot 5}{300} + \frac{(301-v)\cdot 7}{300} + \frac{(301-c)\cdot 9}{300} \quad (3)$$

where h, v and c are times (s) until the start of hemorrhage, vasoconstriction and coagulation, respectively. The formulations were classified according to the following: OII ≤ 0.9 nonirritating; 0.9 < OII ≤ 4.9 weakly irritating; 4.9 < OII ≤ 8.9 moderately irritating; 8.9 < OII ≤ 21 irritating (ICCVAM, 2010).

2.7.2. *In vivo* ocular tolerance

To corroborate the results obtained from the HEM-CAM® test, the formulations (FMT-PLGA-NPs and Isoptoflucon®) were evaluated using primary eye irritation test of Draize (Sánchez-López et al., 2016). For this case, pig eyes (Landrace and Large White) were used, where 50 µL of each sample were instilled in the eye conjunctival sac (n= 6/group) and a gentle massage was applied to ensure circulation of the sample through the eyeball. Possible signs of irritation were observed at the time of instillation and after 1 h of exposure using the untreated contralateral eye as a negative control. Score Draize was determined by direct observation of the anterior segment of the eye and changes in ocular structures involving the cornea (turbidity or opacity), iris and conjunctiva (congestion, chemosis, swelling, and discharge) using Table S.3b Supplementary Material.

2.8. Anti-inflammatory efficacy

The induction of inflammation with the objective of evaluating the anti-inflammatory effect of FMT-PLGA-NPs compared to the commercial drug (Isopotoflucon®) and 0.9 % control group (NaCl), was carried out using pigs (n= 6/group). The study was conducted with the application of 50 µL of 0.5 % sodium arachidonate (SA) dissolved in PBS in the right eye, the left eye was used as control. After 30 minutes of exposure, 50 µL of each formulation were instilled.

Evaluation of inflammation was performed from the application of formulations up to 150 min according to Draize modified scoring system (Sánchez-López et al., 2016).

2.9. Ocular bioavailability

The amounts of drug that permeated from the formulation FMT-PLGA-NPs and Isopotoflucon® were evaluated 4 h after its application. To this end, 50 µL of each formulation were administered to the pig's left eye. The amount of FMT retained from the different parts of the eye (sclera, cornea, aqueous and vitreous humor) was quantified by RP-HPLC.

2.10. Statistical analysis

The multiple comparisons were developed using one-way ANOVA with Tukey post hoc test with a significance of $\alpha < 0.05$ after having confirmed the normality and equality of variances by Bartlett in the groups. All analyzed data were presented as mean ± SD. GraphPad Prism® 6.01 software for windows was used to analyze the data.

3. Results and discussions

3.1. Optimization of the FMT-PLGA-NPs

According to the results obtained from the matrix central composite design (Table S.1 Supplementary Material) it was possible to statistically correlate the effects of the independent variables on Zav and EE ($p < 0.05$). In the first case, Zav was highly influenced by cPLGA and cP188 (Figure 1a). The study showed that as the amount of PLGA in the formulation increased, the NPs increased in size, the opposite happened when the concentration of cP188 increased. Zav's values (141.3-187.8 nm) were within the criteria of the ocular topical administration of nanostructured systems that would not cause irritation (Ali and Lehmussaari, 2006). In the second case, EE, mainly cFMT had a significantly positive effect (Figure 1b), where the ratio of drug concentration and EE is proportional, reaching values close to 100 % (Table S.1 Supplementary Material). The latter could be associated with the fact that cFMT did not have a significant effect ($p = 0.9818$) on Zav (Figure S.1 Supplementary Material), which makes it clear that the load capacity of PLGA had not yet been reached. The other dependent

variables (PI and ZP) were not correlated with any independent variable ($p > 0.05$), however, the PI and ZP values concluded that all the formulations were monodisperse systems (PI ≤ 0.1) and with a low probability that sedimentation would occur (Patel and Agrawal, 2011). Finally, according to the results of the evaluated parameters and their significant effects it was possible to select an optimized nanoparticle formulation (FMT-PLGA-NPs) containing 7.0 $mg{\cdot}mL^{-1}$ of PLGA, 15 $mg{\cdot}mL^{-1}$ of P188 and 1.5 $mg{\cdot}mL^{-1}$ of FMT. Stability studies, physicochemical interactions, release, permeation, eye tolerance, and anti-inflammatory efficacy were carried out to this optimized formulation.

3.2. NPs physicochemical, morphological characterization and EE %

The optimized formulation showed a Zav of 149.1 ± 3.5 nm and a PI of 0.079 ± 0.008, characteristic of monodisperse systems (PI < 0.1), suitable for ocular administration due the fact that there will not be NP populations that have a size greater than 10 µm that could cause ocular irritation associated with particle size (Ali and Lehmussaari, 2006). For the ZP, a negative value (−34.3 ± 1.6 mV) was obtained which was attributed to the PLGA polymer, specifically, to the terminal carboxylic groups of the polymer chain (Stolnik et al., 1995). The high PLGA entrapment capacity used in combination with high liposolubility of the FMT, explains the high value of EE % (99.8 ± 0.2 %) in the optimized formulation. Finally, to corroborate the Zav data coming from the DLS technique, the FMT-PLGA-NPs were visualized by TEM (Figure 2). The TEM images showed that the NPs present similar values observed by DLS and without evidence of aggregation.

3.3. Interaction studies

To demonstrate the crystalline state of the components of the NPs and their interactions with each other, the XRD spectra of FMT-PLGA-NPs, PLGA, P188 and FMT were analyzed (Figure 3a). PLGA shows XRD profiles without any crystalline state signal. The semicrystalline profile of P188 showed peaks at 19.15° and 23.43° (2θ), which were not seen in the FMT-PLGA-NPs. In relation to FMT, it showed a crystalline profile with sharp and intense peaks at 10.38°, 13.79°,

15.32°, 16.32°, 17.00°, 17.60° and 19.60° (2θ). The previous peaks were evidenced in a low intensity in the profile of FMT-PLGA-NPs, due to the fact that FMT was dispersed in the polymer matrix both in crystalline state and molecular dispersion (Panyam et al., 2004).

FTIR analysis was performed to identify the interactions between FMT, P188 and PLGA. According to the analysis of the spectra of each of the components (Figure 3b), there was no evidence of the existence of a covalent bond between the elements that constituted the NPs. The IR spectrum of FMT showed several characteristic peaks, the first at a band of 3384 cm^{-1} given by the signal of the stretching vibration of OH, some peaks from 2994 to 2876 cm^{-1} corresponding to the stretching vibration of CH, some peaks at 1712 and 1654 cm^{-1} due to the stretching vibration the C=O, and finally, stretching vibration product of C=C aromatic to the bands of 1612 and 1601 cm^{-1} (Rodrigues et al., 2009). In the case of the PLGA, it had a characteristic intense band at 1750 cm^{-1} corresponding to stretching vibration of the carbonyl group. Small peaks corresponding to stretching vibration of the alkanes were displayed between the bands 2997 to 2882 cm^{-1}. The stretching vibrations C-O and C-O-O were shown at the bands of 1166 and 1087 cm^{-1}, respectively (Li et al., 2001). In the P188 showed two intense peaks, the first at 2881 cm^{-1} signal given by the stretching vibration of CH and the second at 1097 cm^{-1} corresponding to the stretching vibration of C-O (Yan et al., 2010). The FMT-PLGA-NPs showed comparable profile to PLGA with additional peaks of low intensity corresponding to P188 (C-H) and to FMT (O-H, C-H and C=C).

The DSC thermograms of FMT, FMT-PLGA-NPs, P188 and PLGA are presented in the Figure 3c, in which it is possible to observe an acute peak belonging to the melting transition of P188 with a ΔH= 132.69 $J \cdot g^{-1}$ and a T_{max}= 54.24 °C (Yan et al., 2010). The FMT showed a melting transition characterized by a ΔH= 105.09 $J \cdot g^{-1}$ and with a T_{max}= 291.95 °C that was not present in the profiles of the NPs developed (data not shown) because the P188 has a flash point near 260 °C. The PLGA showed the onset of the glass transition (T_g) at 51.87 °C and in the FMT-

PLGA-NPs at 45.56 °C, this decrease T_g is attributed to the drug-polymer interaction (Abrego et al., 2014; Sánchez-López et al., 2017).

3.4. Biopharmaceutical behavior

3.4.1. *In vitro* release study

The *In vitro* release study of FMT from FMT-PLGA-NPs compared to Isoptoflucon® and Free-FMT was carried out through Franz diffusion cells. In Figure 4, it is possible to observe that after 10 h the Free-FMT formulation released almost 100 % of the FMT. In relation to the commercial solution (Isoptoflucon®), after 24 h amount released was close to 100%. All the above formulations were adjusted to a release profile of first order (Table II), which is characterized by a rapid release followed by a constant release (Fangueiro et al., 2016). FMT-PLGA-NPs, had a release of 60 % of the FMT, with continued increasing and sustained release of the drug, this system was adjusted to a profile of hyperbola order (Sánchez-López et al., 2017). The rapid release of the drug from NPs within the first 10 h was mainly due to the drug that is weakly bound to the most superficial areas of the polymeric matrix. In the sustained and increasing phase of the release of FMT, it could be due to a slow diffusion of the drug due to its affinity within the polymer matrix (Allahyari and Mohit, 2016; Anderson and Shive, 2012).

Table II: Parameters for kinetic models of FMT-PLGA-NPs, free drug solution and Isoptoflucon®.

	Isoptoflucon®		Free FMT		FMT-PLGA-NPs	
Models	**AIC**	**R^2**	**AIC**	**R^2**	**AIC**	**R^2**
Zero Order	117.49	0.62	119.75	0.45	107.51	0.66
First Order	88.29	0.97	68.70	0.99	74.45	0.98
Higuchi	109.21	0.81	113.11	0.68	97.56	0.85
Hyperbola	94.73	0.94	80.54	0.98	74.38	0.99
Korsmeyer-Peppas	n = 0.052		n = 0.030		n = 0.033	
	106.73	0.85	103.98	0.85	91.85	0.91

3.4.2. *Ex vivo* corneal and sclera permeation study

Studies of corneal and scleral permeation were carried out for 6 h (Figure 5). According to Table III, the release of the FMT-PLGA-NP drug is faster and penetrates more at the corneal

345 level than at the scleral level ($p < 0.001$). In the different parameters of scleral permeation (J, K_p and Q_{24}) there were no significant differences between the formulations tested, except for the Q_R, where FMT-PLGA-NPs retain more drug ($p < 0.01$) than the Isoptoflucon®. At corneal permeation level, it was observed that the formulation FMT-PLGA-NPs present significant differences in all parameters ($p < 0.01$) in contrast to the commercial formulation. Comparing 350 the steady-state flux, the drug from the NPs permeated the cornea twice faster than Isoptoflucon®. The previous relation was maintained for the parameters Kp and Q_{24} at the corneal level. The Q_R of FMT-PLGA-NPs was significantly lower in the cornea than the other formulation analyzed. According to the corneal permeation parameters, the NPs formulation has a greater capacity to cross the drug per unit of time (Carvajal-Vidal et al., 2017).

355 **Table III:** FMT sclera and corneal permeation parameters from FMT-PLGA-NPs and Isoptoflucon®.

Tissue	Formulation	J ($ng \cdot h^{-1} \cdot cm^{-2}$)	K_p ($cm \cdot h^{-1}$) ·10	Q_{24} (µg)	Q_R ($\mu g \cdot g^{-1} \cdot cm^{-2}$)
Sclera	Isoptoflucon®	88.87 ± 36.47	5.92 ± 2.43	1.36 ± 0.56	3.26 ± 0.27
	FMT-PLGA-NPs	126.94 ± 3.38	8.43 ± 0.23	1.95 ± 0.05	5.07 ± 0.06 [i]
Cornea	Isoptoflucon®	134.66 ± 17.29	8.98 ± 1.15	2.07 ± 0.27	7.01 ± 0.16
	FMT-PLGA-NPs	305.16 ± 25.41[ii]	20.34 ± 1.69 [ii]	4.69 ± 0.39 [ii]	2.73 ± 0.30 [i]

Letters represent statistical significance: [i] $p < 0.01$ and [ii] $p < 0.001$. J, steady-state flux; K_p, permeability coefficient; Q_{24}, permeated amount at 24 h; Q_R, retained amount.

3.5. Stability analysis of NPs

360 In accordance with the Figure 6a, it is possible to observe that the designed NPs present high stability after one month a storage temperature at 4 °C. The previously described also happened with the NPs at a storage temperature at 25 °C until the course of 15 days (Figure 6b). This stability is associated with the high ZP of the NPs (approximately -30 mV) that allow them to avoid flocculation and precipitation (Patel and Agrawal, 2011). After 30 days, the NPs 365 stored at 25 °C begin to show signs of instability, due to the increase in temperature-dependent solubility of P188. This causes the release of P188 absorbed on the surface of the NP, gradually losing the ZP that causes the agglomeration and later, the flocculation of the nanostructured system (Fredenberg et al., 2011; Storm et al., 1995).

3.6. Ocular tolerance

3.6.1. *In vitro* ocular tolerance

The HET-CAM was tested on optimized NPs compared to the commercial drug (Table S.2 Supplementary Material). For this, the assay was validated by evaluating a positive and negative control. The positive control, 0.1 M NaOH, produced a severe hemorrhage (Figure S.2a Supplementary Material), classifying this solution as irritating. In contrast, the negative control did not produce any type of injury, categorizing it as nonirritating (Figure S.2b Supplementary Material). In relation to the formulation of FMT-PLGA-NPs and Isoptoflucon® showed a high ocular tolerance with an OII ≤ 0.9 during the whole experiment, classifying it as nonirritating (Figure S.2c and Figure S.2d Supplementary Material).

3.6.2. *In vivo* ocular tolerance

The topical administration in the eyes of the pigs showed no signs of irritation in the different structures (cornea, iris and conjunctiva) evaluated (Figure S.3 Supplementary Material). A value of OII = 0 was obtained both for the commercial formulation and for the optimized NPs, classifying them as nonirritating (Table S.3c Supplementary Material). These results agreed with the data obtained from the HET-CAM® assay and other studies (Abrego et al., 2015; Parra et al., 2016).

3.7. Anti-inflammatory efficacy assay

A study of anti-inflammatory efficacy was developed with the aim to determine the anti-inflammatory capacity in contrast with a commercial formulation (Isoptoflucon®) in an acute treatment. According to Figure 7, both the formulation Isoptoflucon® and the FMT-PLGA-NPs showed a significant anti-inflammatory effect from the first 30 minutes of exposure when compared with the positive control (SA). When comparing the anti-inflammatory effect between the formulations, it is evident that there is a significant difference ($p < 0.01$) of a greater anti-inflammatory effect of FMT-PLGA-NPs throughout the treatment. The above difference is explained by the information from the corneal permeation studies performed.

The FMT-PLGA-NPs had a greater and faster permeation of the drug, reflecting a faster and more effective anti-inflammatory effect in contrast to Isoptoflucon®. The nanostructured system gives the drug greater bioavailability at the corneal level and with the ability to reach deeper tissues such as vitreous and retina, making it useful for posterior uveitis (Bisht et al., 2017).

3.8. Ocular bioavailability

In order to determine the bioavailability of FMT in the different pig eye structures, the formulation of FMT-PLGA-NPs and Isoptoflucon® were instilled for an exposure period of 4 h. The amount of FMT from FMT-PLGA-NPs in aqueous humor was 11.16 ± 1.31 $\mu g \cdot mL^{-1}$ significantly higher ($p < 0.0001$) to the other cavities. The amounts found in cornea, sclera and vitreous were 1.36 ± 0.12 $\mu g \cdot mL^{-1}$, 0.82 ± 0.09 $\mu g \cdot mL^{-1}$ and 0.06 ± 0.03 $\mu g \cdot mL^{-1}$, respectively. The amount of drug found in the aqueous humor correlates with the data on permeation and anti-inflammatory efficacy. The *ex vivo* permeation study showed that the formulation FMT-PLGA-NPs permeated greater amount of drug per unit of time with a lower retention than the other formulations tested, justifying that the NPs had a greater anti-inflammatory effect to the commercial formulation in the *in vivo* study. In this study, it was evidenced that the drug accumulates in the aqueous humor slowly releasing the drug to the deeper tissues such as the vitreous (Kalam and Alshamsan, 2017; Warsi et al., 2014). In the case of Isoptoflucon®, no amounts of the drug were detected in any of the structures of the pig's eye with the quantification method used.

4. CONCLUSIONS

In the current study FMT-loaded PLGA NPs have been developed by solvent displacement technique, and in turn optimized using DoE, obtaining a formulation with physicochemical (Zav, ZP, PI and EE) and morphological characteristics suitable for ocular administration.

Through the Zav information delivered by the DLS and TEM technique (Zav < 200 nm), the optimized formulation would not cause ocular irritation due to particle size. The formulation was submitted to the study of ocular tolerance *in vitro* and *in vivo* to argue the previously described, in which it was demonstrated that there is a high ocular tolerance of FMT-PLGA-NPs. The interaction studies showed that the drug is contained within the polymer matrix in the form of dispersion system and that the different components that make up the NPs do not have chemical interactions or strong covalent bonds that could affect pharmacology activity of FMT. The formulation FMT-PLGA-NPs shows a bimodal behavior in which the first 10 h presents a rapid release of the drug followed with increasing and sustained release of the drug. The permeation study allowed us to show that FMT-PLGA-NPs have a higher permeability at corneal level with a low corneal retention of the drug compared to the commercial formulation ($p < 0.01$). The low corneal permeation was corroborated by the bioavailability study, which showed that there is a greater amount of drug in the aqueous humor than in the other ocular structures, demonstrating that the system has the capacities to reach the vitreous. In the stability study of NPs, it is established that the system maintains its properties without signs of flocculation and/or sedimentation at a storage temperature of 4 °C, at higher temperatures they could solubilize the P188 causing the loss of ZP causing the flocculation of the NPs. In the *in vivo* study of anti-inflammatory efficacy, the permeation and dialysis data were corroborated, in which it was evidenced that the FMT-PLGA-NPs have a greater anti-inflammatory effect than the commercial formulation during the whole experiment. Considering all the aspects analyzed, the formulation developed would be useful for the acute and chronic treatment of ocular inflammatory conditions with the ability to reach the posterior segment.

ACKNOWLEDGMENTS

The authors would like to thank to the Spanish Ministry of Science and Innovation (MAT2014-59134R) and to the National Commission for Scientific and Technological Research of Chile

(CONICYT) 2014-72150367 for a doctoral grant (R.C.G.P). Thanks to Dr. Alvaro Gimeno and Lidia Gómez for their help in the *in vivo* studies.

REFERENCES

Abrego, G., Alvarado, H., Souto, E.B., Guevara, B., Bellowa, L.H., Parra, A., Calpena, A., Garcia, M.L., 2015. Biopharmaceutical profile of pranoprofen-loaded PLGA nanoparticles containing hydrogels for ocular administration. Eur. J. Pharm. Biopharm. 95, 261–70. https://doi.org/10.1016/j.ejpb.2015.01.026

Abrego, G., Alvarado, H.L., Egea, M.A., Gonzalez-Mira, E., Calpena, A.C., Garcia, M.L., 2014. Design of nanosuspensions and freeze-dried PLGA nanoparticles as a novel approach for ophthalmic delivery of pranoprofen. J. Pharm. Sci. 103, 3153–64. https://doi.org/10.1002/jps.24101

Ali, Y., Lehmussaari, K., 2006. Industrial perspective in ocular drug delivery. Adv. Drug Deliv. Rev. 58, 1258–1268. https://doi.org/10.1016/J.ADDR.2006.07.022

Allahyari, M., Mohit, E., 2016. Peptide/protein vaccine delivery system based on PLGA particles. Hum. Vaccin. Immunother. 12, 806–28. https://doi.org/10.1080/21645515.2015.1102804

Anderson, J.M., Shive, M.S., 2012. Biodegradation and biocompatibility of PLA and PLGA microspheres. Adv. Drug Deliv. Rev. 64, 72–82. https://doi.org/10.1016/j.addr.2012.09.004

Bielory, B.P., Perez, V.L., Bielory, L., 2010. Treatment of seasonal allergic conjunctivitis with ophthalmic corticosteroids: in search of the perfect ocular corticosteroids in the treatment of allergic conjunctivitis. Curr. Opin. Allergy Clin. Immunol. 10, 469–477. https://doi.org/10.1097/ACI.0b013e32833dfa28

Bisht, R., Mandal, A., Jaiswal, J.K., Rupenthal, I.D., 2017. Nanocarrier mediated retinal drug

delivery: overcoming ocular barriers to treat posterior eye diseases. Wiley Interdiscip. Rev. Nanomedicine Nanobiotechnology e1473. https://doi.org/10.1002/wnan.1473

Cañadas, C., Alvarado, H., Calpena, A.C., Silva, A.M., Souto, E.B., García, M.L., Abrego, G., 2016. In vitro, ex vivo and in vivo characterization of PLGA nanoparticles loading pranoprofen for ocular administration. Int. J. Pharm. 511, 719–727. https://doi.org/10.1016/j.ijpharm.2016.07.055

Cano, A., Ettcheto, M., Espina, M., Auladell, C., Calpena, A.C., Folch, J., Barenys, M., Sánchez-López, E., Camins, A., García, M.L., 2018. Epigallocatechin-3-gallate loaded PEGylated-PLGA nanoparticles: A new anti-seizure strategy for temporal lobe epilepsy. Nanomedicine Nanotechnology, Biol. Med. 14, 1073–1085. https://doi.org/10.1016/J.NANO.2018.01.019

Carvajal-Vidal, P., Mallandrich, M., García, M., Calpena, A., 2017. Effect of different skin penetration promoters in halobetasol propionate permeation and retention in human skin. Int. J. Mol. Sci. 18, 2475. https://doi.org/10.3390/ijms18112475

Chen, P.-Q., Han, X.-M., Zhu, Y.-N., Xu, J., 2016. Comparison of the anti-inflammatory effects of fluorometholone 0.1% combined with levofloxacin 0.5% and tobramycin/dexamethasone eye drops after cataract surgery. Int. J. Ophthalmol. 9, 1619–1623. https://doi.org/10.18240/ijo.2016.11.13

Danhier, F., Ansorena, E., Silva, J.M., Coco, R., Le Breton, A., Préat, V., 2012. PLGA-based nanoparticles: an overview of biomedical applications. J. Control. Release 161, 505–22. https://doi.org/10.1016/j.jconrel.2012.01.043

Diebold, Y., Calonge, M., 2010. Applications of nanoparticles in ophthalmology. Prog. Retin. Eye Res. 29, 596–609. https://doi.org/10.1016/j.preteyeres.2010.08.002

Fangueiro, J.F., Calpena, A.C., Clares, B., Andreani, T., Egea, M.A., Veiga, F.J., Garcia, M.L., Silva,

A.M., Souto, E.B., 2016. Biopharmaceutical evaluation of epigallocatechin gallate-loaded cationic lipid nanoparticles (EGCG-LNs): In vivo, in vitro and ex vivo studies. Int. J. Pharm. 502, 161–169. https://doi.org/10.1016/j.ijpharm.2016.02.039

Fessi, H., Puisieux, F., Devissaguet, J.P., Ammoury, N., Benita, S., 1989. Nanocapsule formation by interfacial polymer deposition following solvent displacement. Int. J. Pharm. 55, R1–R4. https://doi.org/10.1016/0378-5173(89)90281-0

Fredenberg, S., Wahlgren, M., Reslow, M., Axelsson, A., 2011. The mechanisms of drug release in poly(lactic-co-glycolic acid)-based drug delivery systems—A review. Int. J. Pharm. 415, 34–52. https://doi.org/10.1016/J.IJPHARM.2011.05.049

Gause, S., Hsu, K.-H., Shafor, C., Dixon, P., Powell, K.C., Chauhan, A., 2016. Mechanistic modeling of ophthalmic drug delivery to the anterior chamber by eye drops and contact lenses. Adv. Colloid Interface Sci. 233, 139–154. https://doi.org/10.1016/J.CIS.2015.08.002

Guengerich, F.P., 2017. Intersection of the roles of cytochrome P450 enzymes with xenobiotic and endogenous substrates: relevance to toxicity and drug interactions. Chem. Res. Toxicol. 30, 2–12. https://doi.org/10.1021/acs.chemrestox.6b00226

ICCVAM, 2010. ICCVAM-recommended test method protocol: Hen's Egg test – chorioallantoic membrane (HET-CAM) test method. NIH Publ. N° 10-7553 B29–B38.

ICH, 2005. International Conference on Harmonisation of technical requirements for registration of pharmaceuticals for human use (ICH), ICH Q2 (R1) Validation of Analytical Procedures: Text and Methodology.

Kalam, M.A., Alshamsan, A., 2017. Poly (d, l-lactide-co-glycolide) nanoparticles for sustained release of tacrolimus in rabbit eyes. Biomed. Pharmacother. 94, 402–411. https://doi.org/10.1016/J.BIOPHA.2017.07.110

Kapoor, D.N., Bhatia, A., Kaur, R., Sharma, R., Kaur, G., Dhawan, S., 2015. PLGA: a unique polymer for drug delivery. Ther. Deliv. 6, 41–58. https://doi.org/10.4155/tde.14.91

Klose, D., Delplace, C., Siepmann, J., 2011. Unintended potential impact of perfect sink conditions on PLGA degradation in microparticles. Int. J. Pharm. 404, 75–82. https://doi.org/10.1016/J.IJPHARM.2010.10.054

Li, Y.-P., Pei, Y.-Y., Zhang, X.-Y., Gu, Z.-H., Zhou, Z.-H., Yuan, W.-F., Zhou, J.-J., Zhu, J.-H., Gao, X.-J., 2001. PEGylated PLGA nanoparticles as protein carriers: synthesis, preparation and biodistribution in rats. J. Control. Release 71, 203–211. https://doi.org/10.1016/S0168-3659(01)00218-8

Makadia, H.K., Siegel, S.J., 2011. Poly Lactic-co-Glycolic Acid (PLGA) as biodegradable controlled drug delivery carrier. Polymers (Basel). 3, 1377–1397. https://doi.org/10.3390/polym3031377

Nekkanti, V., Marwah, A., Pillai, R., 2015. Media milling process optimization for manufacture of drug nanoparticles using design of experiments (DOE). Drug Dev. Ind. Pharm. 41, 124–130. https://doi.org/10.3109/03639045.2013.850709

Panyam, J., William, D., Dash, A., Leslie-Pelecky, D., Labhasetwar, V., 2004. Solid-state solubility influences encapsulation and release of hydrophobic drugs from PLGA/PLA nanoparticles. J. Pharm. Sci. 93, 1804–1814. https://doi.org/10.1002/jps.20094

Parra, A., Clares, B., Rosselló, A., Garduño-Ramírez, M.L., Abrego, G., García, M.L., Calpena, A.C., 2016. Ex vivo permeation of carprofen from nanoparticles: a comprehensive study through human, porcine and bovine skin as anti-inflammatory agent. Int. J. Pharm. 501, 10–17. https://doi.org/10.1016/j.ijpharm.2016.01.056

Patel, V.R., Agrawal, Y.K., 2011. Nanosuspension: An approach to enhance solubility of drugs. J. Adv. Pharm. Technol. Res. 2, 81–7. https://doi.org/10.4103/2231-4040.82950

Ramos Yacasi, G.R., García López, M.L., Espina García, M., Parra Coca, A., Calpena Campmany, A.C., 2016. Influence of freeze-drying and γ-irradiation in preclinical studies of flurbiprofen polymeric nanoparticles for ocular delivery using d-(+)-trehalose and polyethylene glycol. Int. J. Nanomedicine 11, 4093–106. https://doi.org/10.2147/IJN.S105606

Rodrigues, L.B., Leite, H.F., Yoshida, M.I., Saliba, J.B., Junior, A.S.C., Faraco, A.A.G., 2009. In vitro release and characterization of chitosan films as dexamethasone carrier. Int. J. Pharm. 368, 1–6. https://doi.org/10.1016/J.IJPHARM.2008.09.047

Sánchez-López, E., Egea, M.A., Cano, A., Espina, M., Calpena, A.C., Ettcheto, M., Camins, A., Souto, E.B., Silva, A.M., García, M.L., 2016. PEGylated PLGA nanospheres optimized by design of experiments for ocular administration of dexibuprofen —in vitro, ex vivo and in vivo characterization. Colloids Surfaces B Biointerfaces 145, 241–250. https://doi.org/10.1016/j.colsurfb.2016.04.054

Sánchez-López, E., Ettcheto, M., Egea, M.A., Espina, M., Calpena, A.C., Folch, J., Camins, A., García, M.L., 2017. New potential strategies for Alzheimer's disease prevention: pegylated biodegradable dexibuprofen nanospheres administration to APPswe/PS1dE9. Nanomedicine 13, 1171–1182. https://doi.org/10.1016/j.nano.2016.12.003

Shokoohi-Rad, S., Daneshvar, R., Jafarian-Shahri, M., Rajaee, P., 2017. Comparison between betamethasone, fluorometholone and loteprednol etabonate on intraocular pressure in patients after keratorefractive surgery. J. Curr. Ophthalmol. 1–6. https://doi.org/10.1016/J.JOCO.2017.11.008

Siddique, M.I., Katas, H., Iqbal Mohd Amin, M.C., Ng, S.-F., Zulfakar, M.H., Buang, F., Jamil, A., 2015. Minimization of local and systemic adverse effects of topical glucocorticoids by nanoencapsulation: in vivo safety of Hydrocortisone-Hydroxytyrosol loaded chitosan nanoparticles. J. Pharm. Sci. 104, 4276–86. https://doi.org/10.1002/jps.24666

Silva-Abreu, M., Calpena, A.C., Espina, M., Silva, A.M., Gimeno, A., Egea, M.A., García, M.L., 2018. Optimization, biopharmaceutical profile and therapeutic efficacy of pioglitazone-loaded PLGA-PEG nanospheres as a novel strategy for ocular inflammatory disorders. Pharm. Res. 35, 11. https://doi.org/10.1007/s11095-017-2319-8

Stolnik, S., Garnett, M., Davies, M., Illum, L., Bousta, M., Vert, M., Davis, S., 1995. The colloidal properties of surfactant-free biodegradable nanospheres from poly(β-malic acid-co-benzyl malate)s and poly(lactic acid-co-glycolide). Colloids Surfaces A Physicochem. Eng. Asp. 97, 235–245. https://doi.org/10.1016/0927-7757(95)03081-N

Storm, G., Belliot, S.O., Daemen, T., Lasic, D.D., 1995. Surface modification of nanoparticles to oppose uptake by the mononuclear phagocyte system. Adv. Drug Deliv. Rev. 17, 31–48. https://doi.org/10.1016/0169-409X(95)00039-A

Tahara, K., Karasawa, K., Onodera, R., Takeuchi, H., 2017. Feasibility of drug delivery to the eye's posterior segment by topical instillation of PLGA nanoparticles. Asian J. Pharm. Sci. 12, 394–399. https://doi.org/10.1016/J.AJPS.2017.03.002

USP 29-NF 24, 2006. United States Pharmacopeia and National Formulary (USP 39-NF 34). United States Pharmacopeial Convention., Rockville, Md.

Warsi, M.H., Anwar, M., Garg, V., Jain, G.K., Talegaonkar, S., Ahmad, F.J., Khar, R.K., 2014. Dorzolamide-loaded PLGA/vitamin E TPGS nanoparticles for glaucoma therapy: Pharmacoscintigraphy study and evaluation of extended ocular hypotensive effect in rabbits. Colloids Surfaces B Biointerfaces 122, 423–431. https://doi.org/10.1016/j.colsurfb.2014.07.004

Yan, F., Zhang, C., Zheng, Y., Mei, L., Tang, L., Song, C., Sun, H., Huang, L., 2010. The effect of poloxamer 188 on nanoparticle morphology, size, cancer cell uptake, and cytotoxicity. Nanomedicine 6, 170–8. https://doi.org/10.1016/j.nano.2009.05.004

Yasin, M.N., Svirskis, D., Seyfoddin, A., Rupenthal, I.D., 2014. Implants for drug delivery to the posterior segment of the eye: a focus on stimuli-responsive and tunable release systems. J. Control. Release 196, 208–221. https://doi.org/10.1016/j.jconrel.2014.09.030

Figure 1a

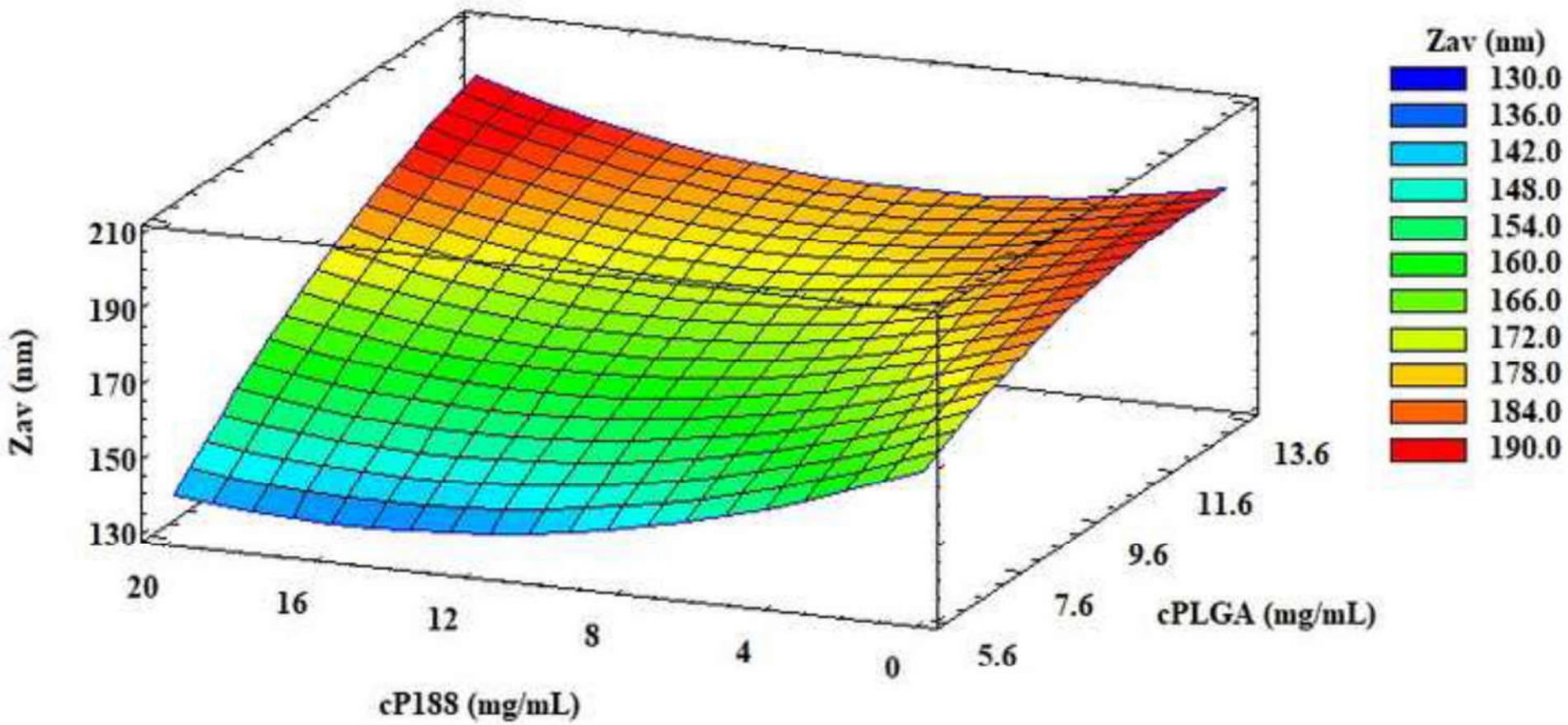
Zav (nm)
130.0
136.0
142.0
148.0
154.0
160.0
166.0
172.0
178.0
184.0
190.0
Zav (nm)
210
190
170
150
130
20
16
12
8
4
0
cP188 (mg/mL)
5.6
7.6
9.6
11.6
13.6
cPLGA (mg/mL)

Figure 1b

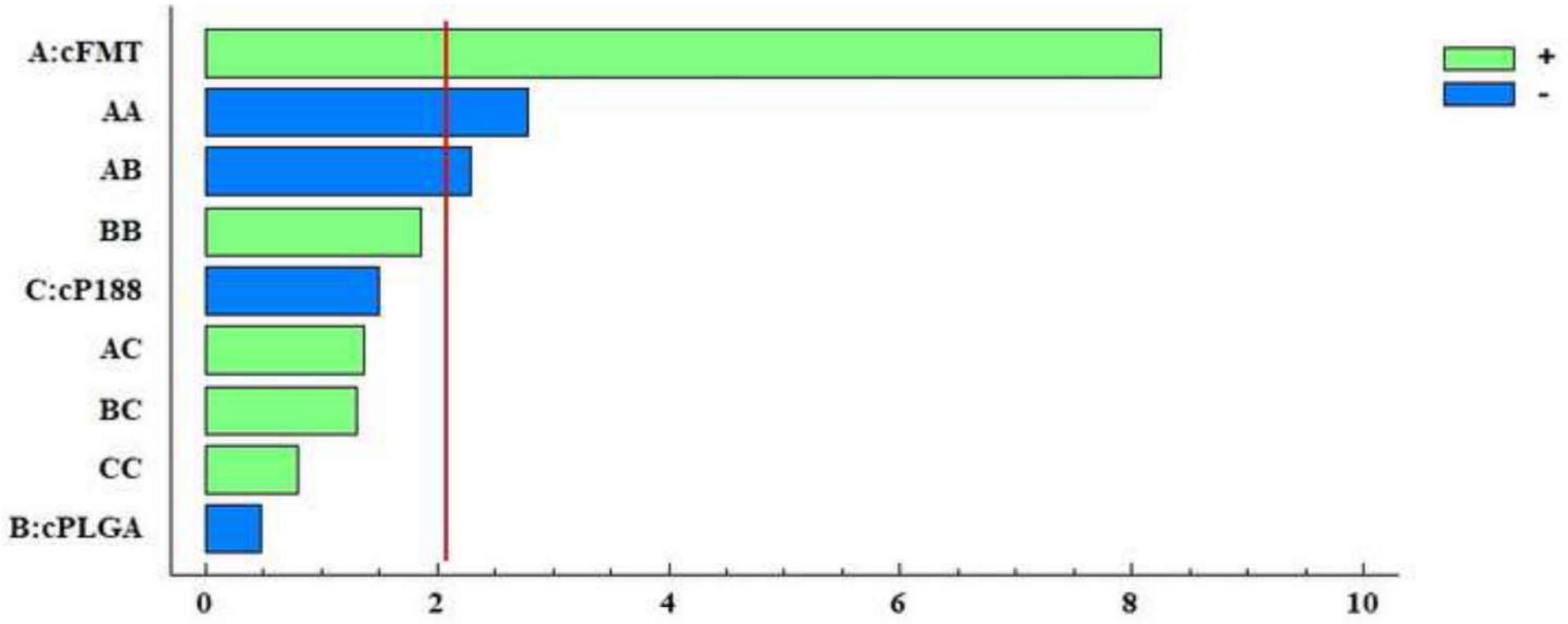

Figure 2

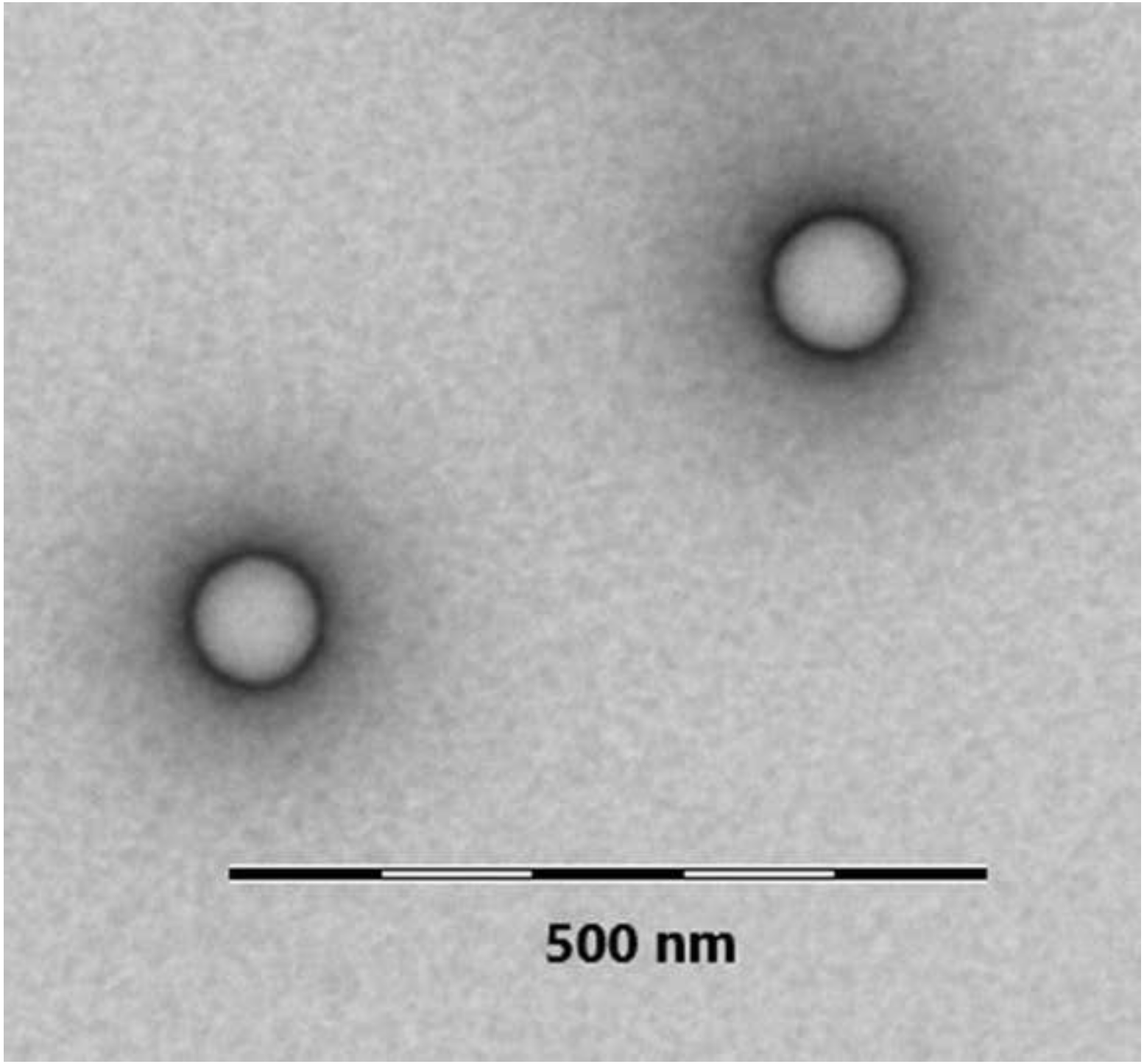

Figure 3a

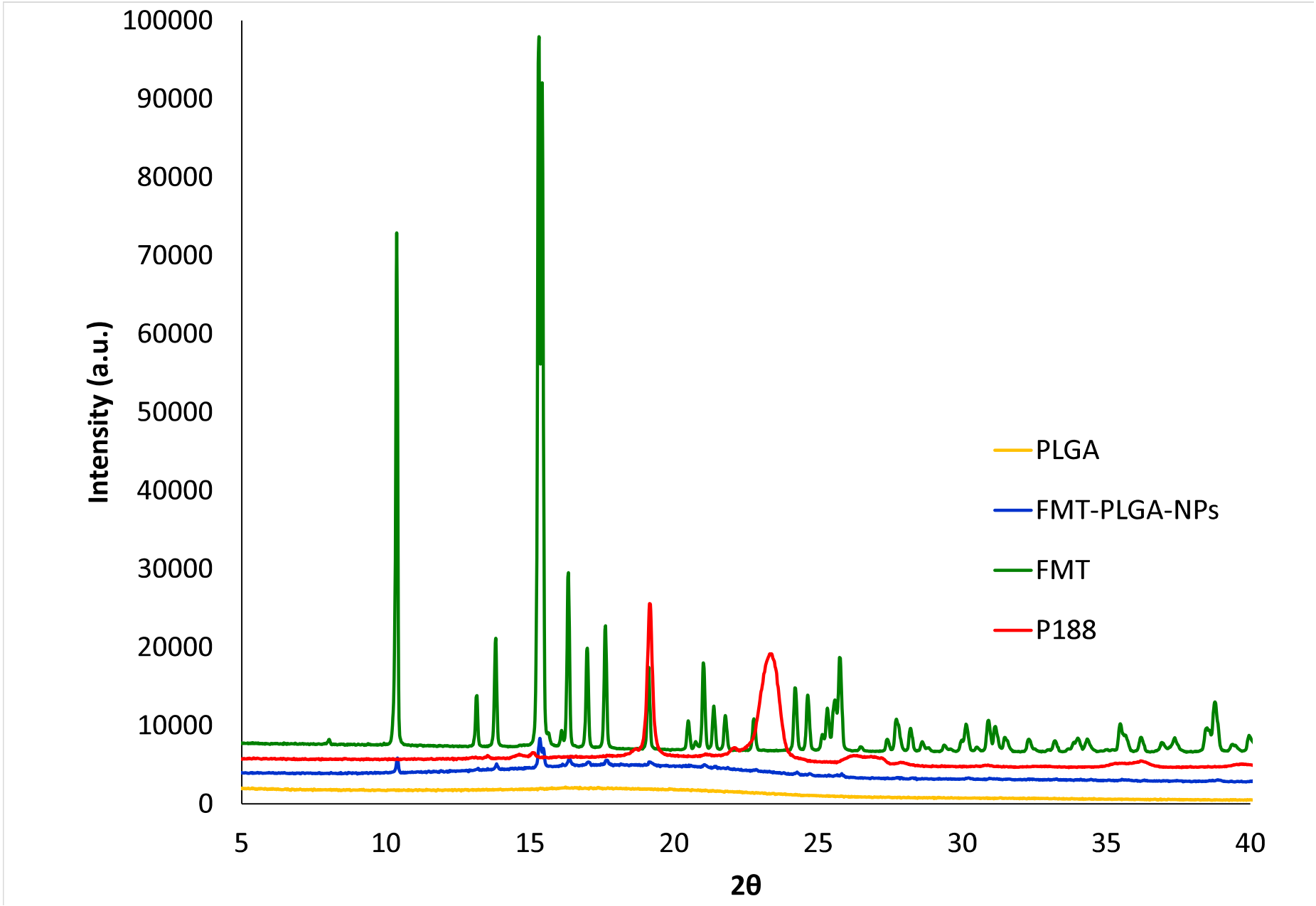
100000
90000
80000
70000
60000
50000
40000
30000
20000
10000
0
Intensity (a.u.)
5
10
15
20
25
30
35
40
2θ
PLGA
FMT-PLGA-NPs
FMT
P188

Figure 3b

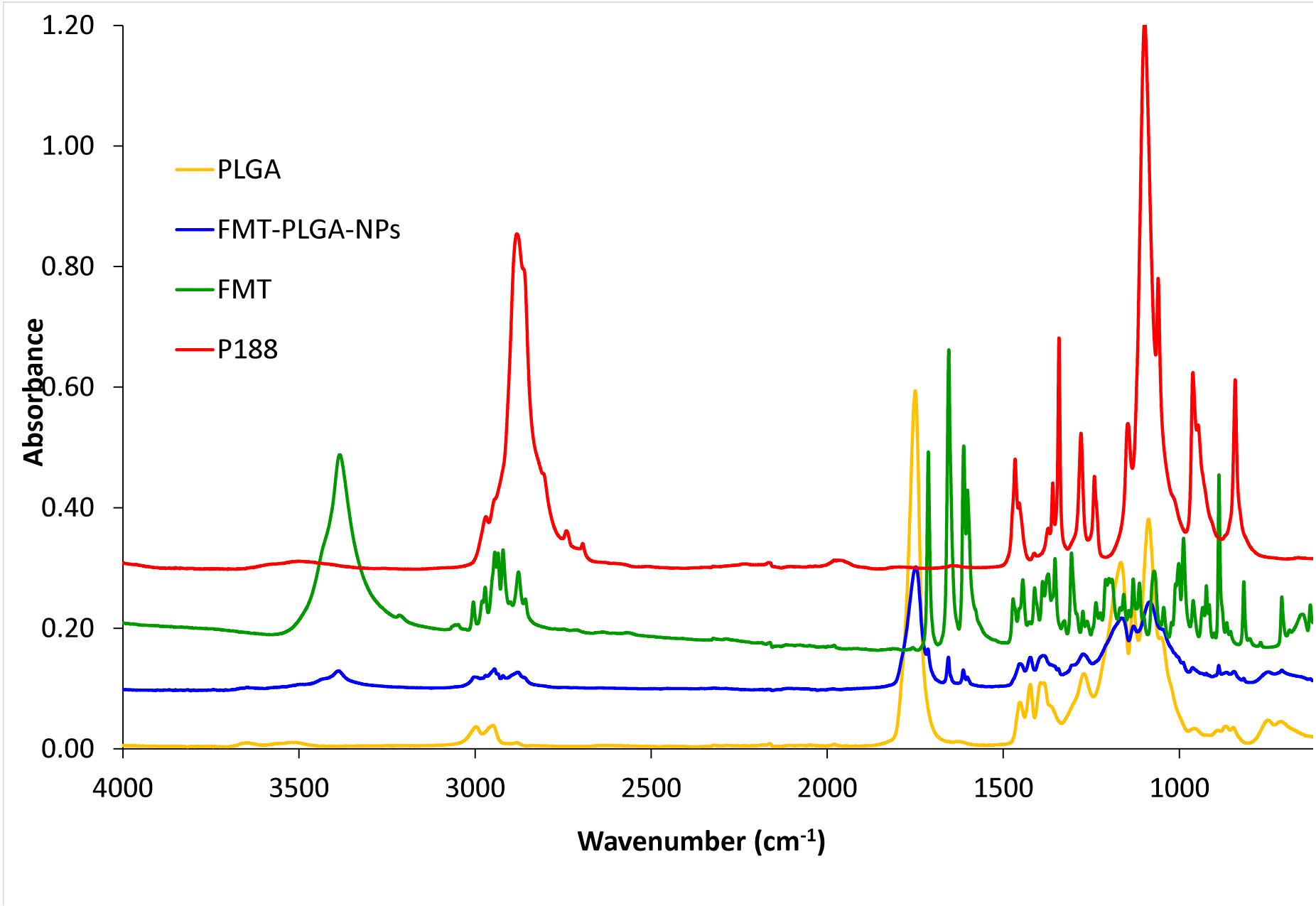
1.20
1.00
0.80
0.60
0.40
0.20
0.00
Absorbance
PLGA
FMT-PLGA-NPs
FMT
P188
4000
3500
3000
2500
2000
1500
1000
Wavenumber (cm-1)

Figure 3c

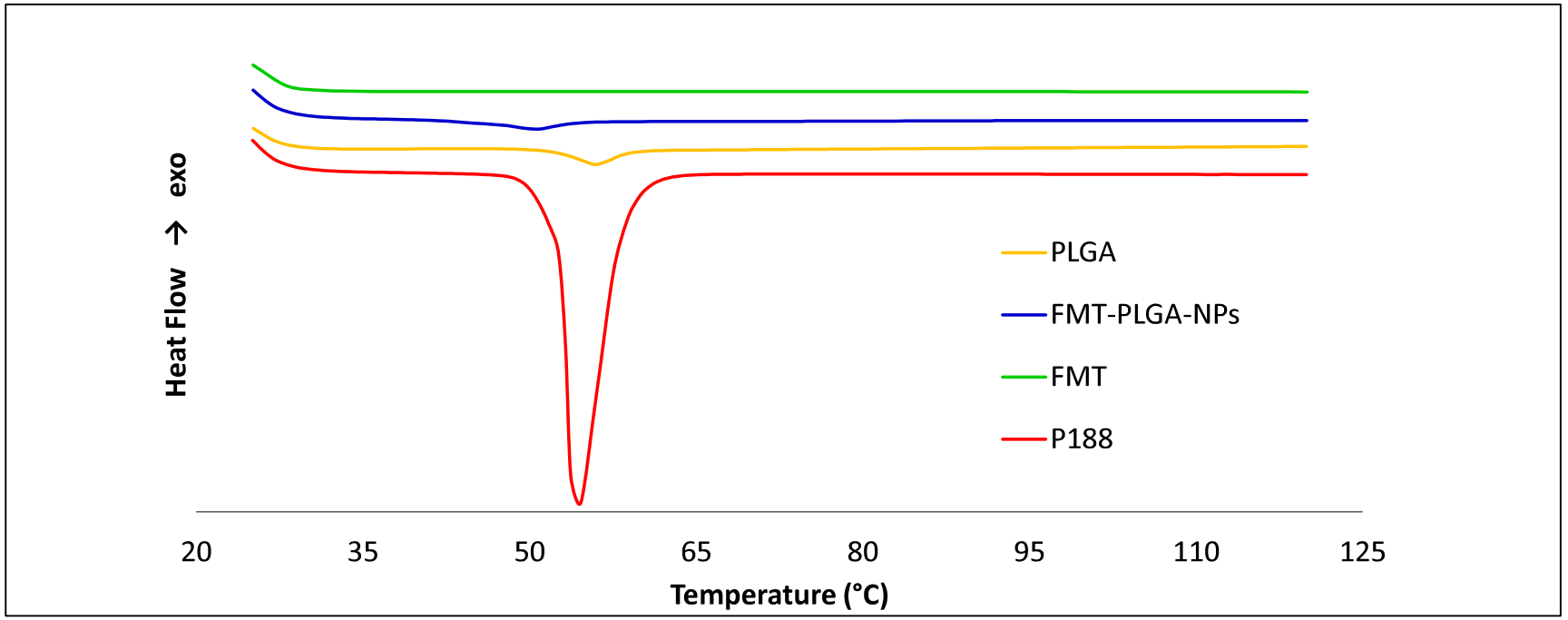
Heat Flow → exo
PLGA
FMT-PLGA-NPs
FMT
P188
20
35
50
65
80
95
110
125
Temperature (°C)

Figure 4

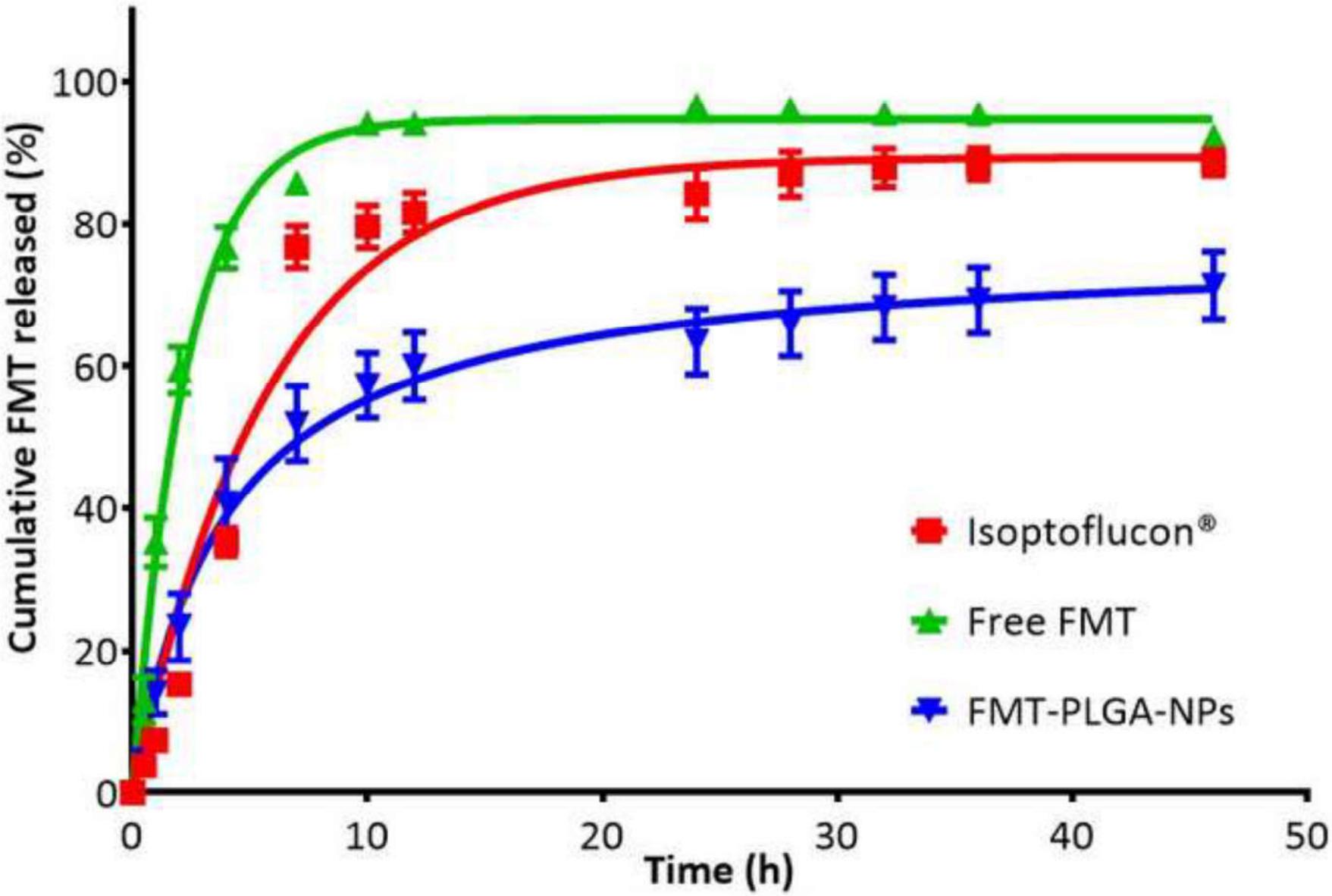
Cumulative FMT released (%)
100
80
60
40
20
0
0
10
20
30
40
50
Time (h)
Isoptoflucon®
Free FMT
FMT-PLGA-NPs

Figure 5a

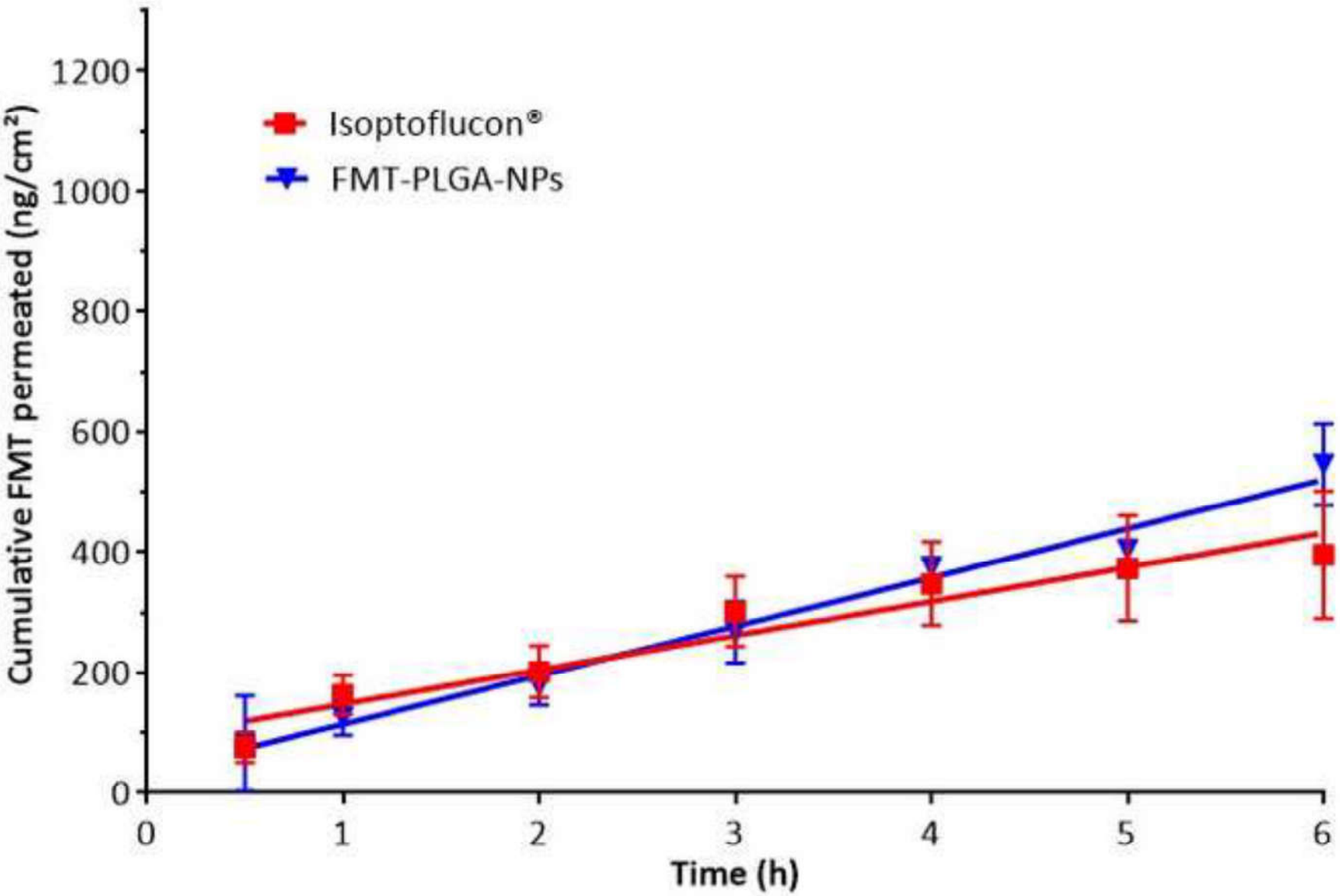
Isoptoflucon®
FMT-PLGA-NPs
Cumulative FMT permeated (ng/cm²)
1200
1000
800
600
400
200
0
0
1
2
3
4
5
6
Time (h)

Figure 5b

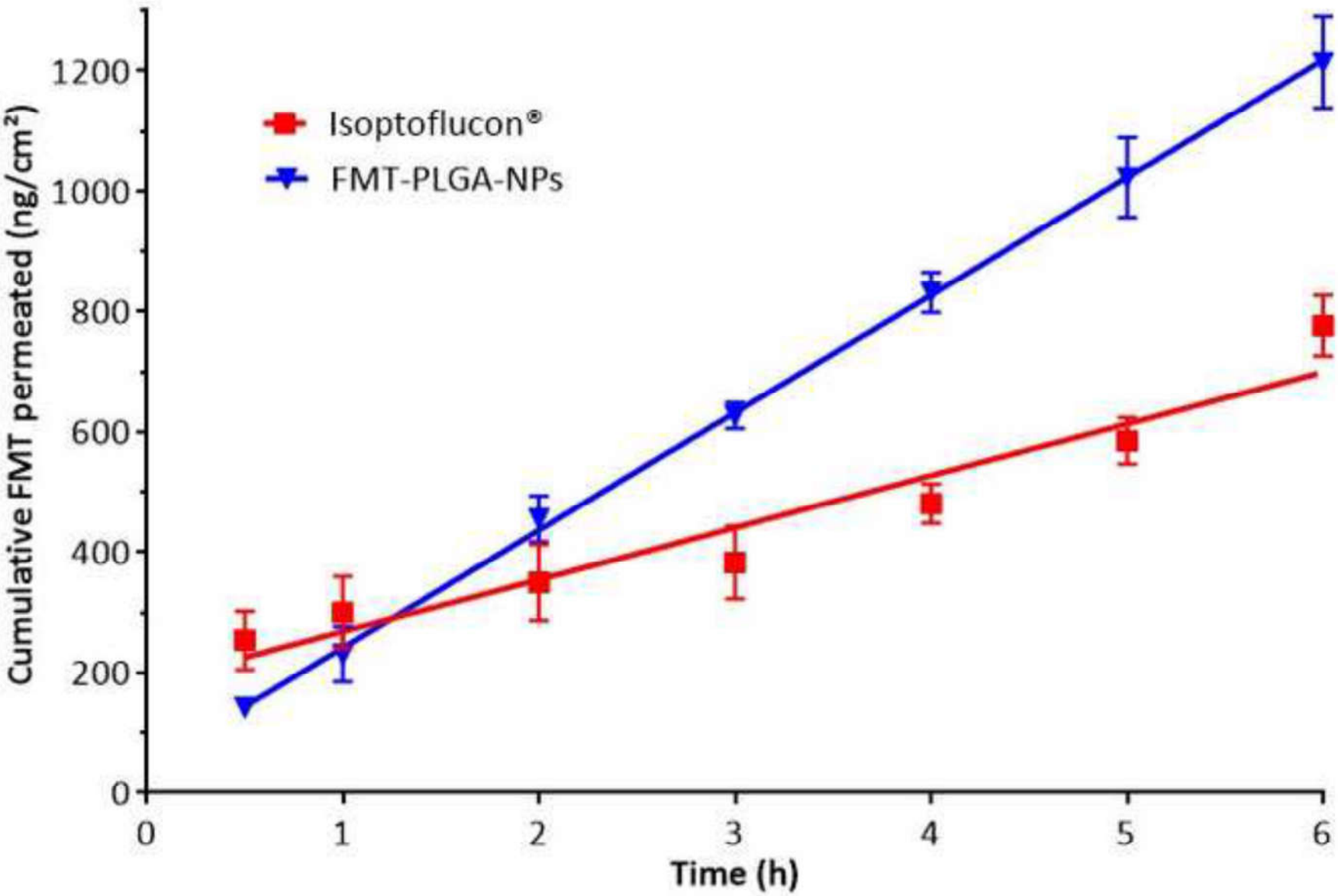
Isoptoflucon®
FMT-PLGA-NPs
Cumulative FMT permeated (ng/cm²)
1200
1000
800
600
400
200
0
0
1
2
3
4
5
6
Time (h)

Figure 6a

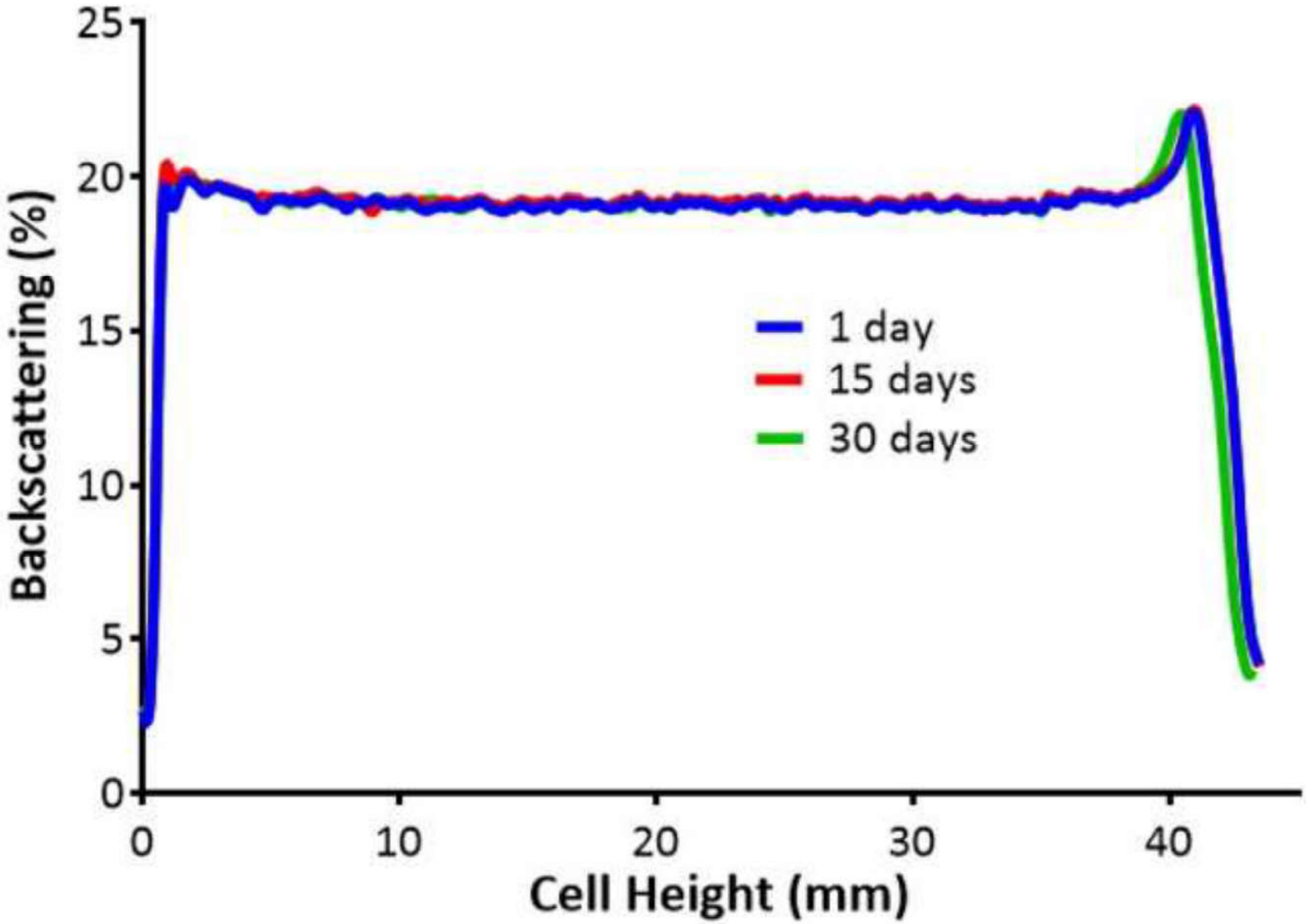
Backscattering (%)
25
20
15
10
5
0
0
10
20
30
40
Cell Height (mm)
1 day
15 days
30 days

Figure 6b

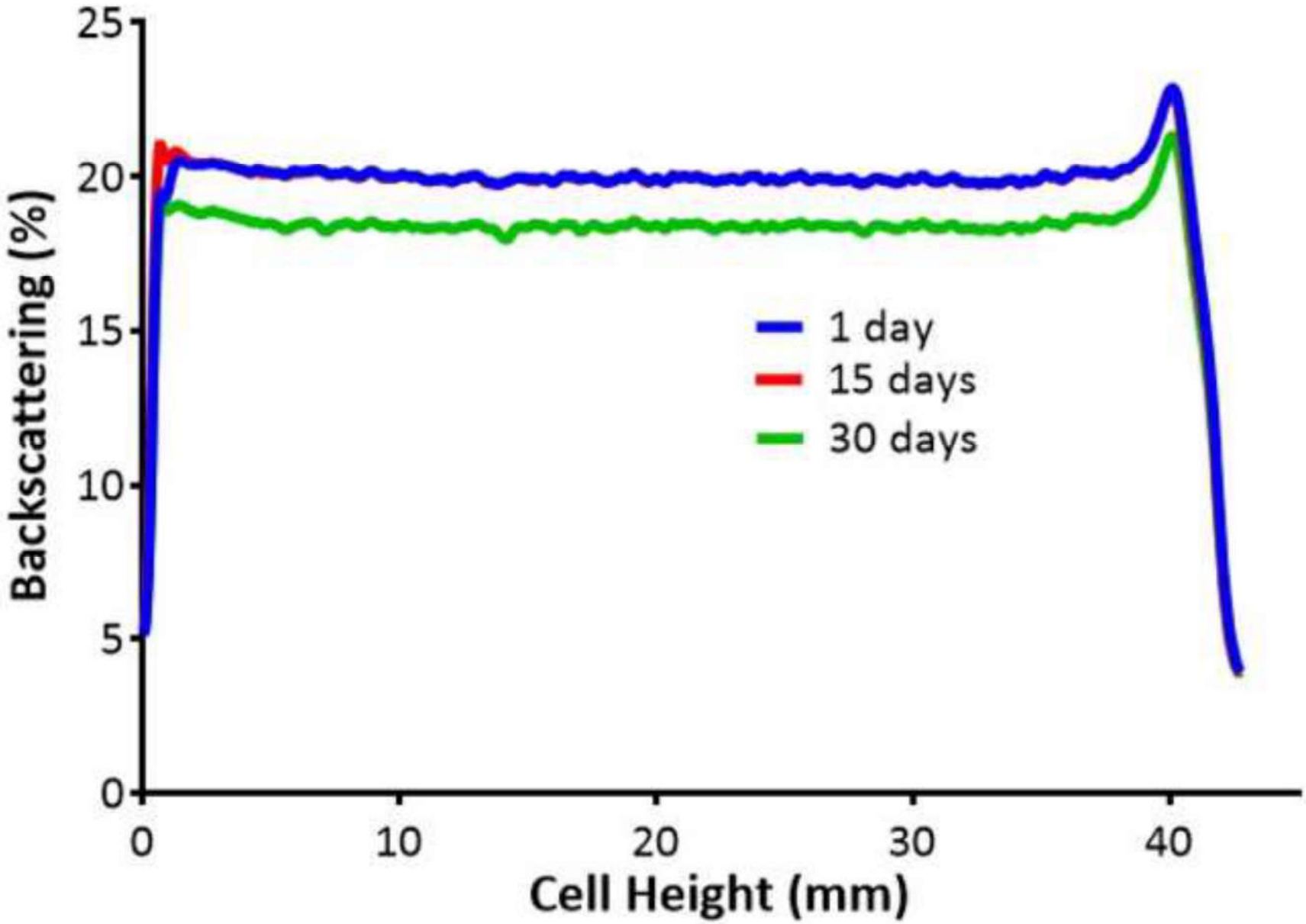
Backscattering (%)
25
20
15
10
5
0
0
10
20
30
40
Cell Height (mm)
1 day
15 days
30 days

Figure 7

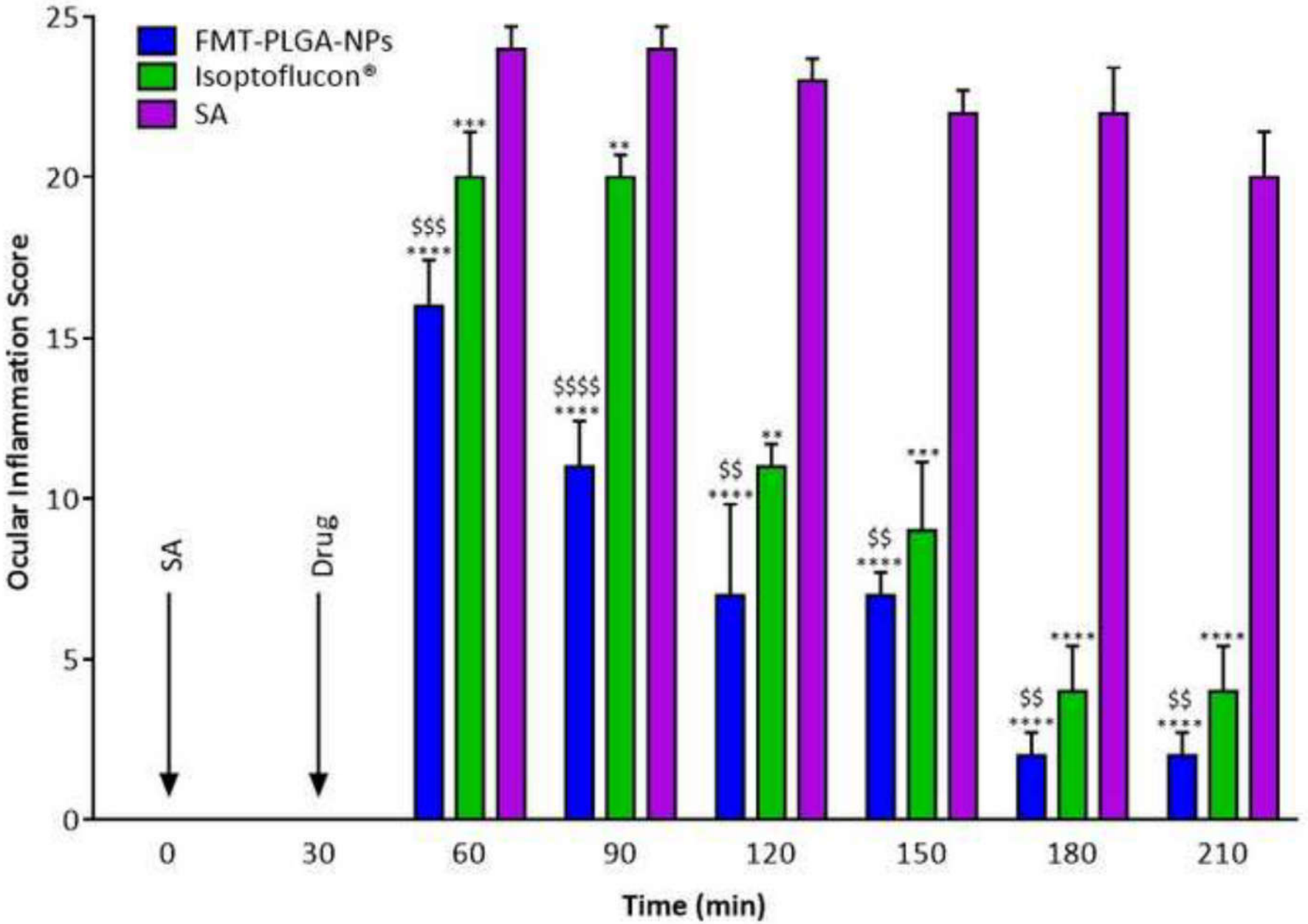
FMT-PLGA-NPs
Isoptoflucon®
SA
Ocular Inflammation Score
25
20
15
10
5
0
SA
Drug
0
30
60
90
120
150
180
210
Time (min)
$$$
$$$$
$$
$$

Figure captions

Figure 1. Optimization of the FMT-PLGA-NPs. (a) Zav surface response at a fix 1.5 $mg \cdot mL^{-1}$ of FMT, (b) Pareto' diagram of the analyzed effect on EE %.

Figure 2. TEM of FMT-PLGA-NPs

Figure 3. Interactions studies of FMT-PLGA-NPs and NPs components (a) XRD patterns, (b) FTIR spectra, (c) DSC.

Figure 4. *In vitro* profile release of FMT-PLGA-NPs (adjust to hyperbola equation) against free FMT and Isoptoflucon® (adjust to first order).

Figure 5. *Ex vivo* permeation profile of FMT-PLGA-NPs compared with Isoptoflucon®. (a) Scleral permeation (b) Corneal permeation.

Figure 6. FMT-PLGA-NPs backscattering profile. (a) Storage temperature at 4 °C, (b) Storage temperature at 25 °C.

Figure 7. Comparation of anti-inflammatory efficacy of FMT-PLGA-NPs and Isoptoflucon. Values are expressed as mean ± SD; ** $p < 0.01$, *** $p < 0.001$, and **** $p < 0.0001$ significantly lower than the inflammatory effect induced by SA; $$ $p < 0.01$, $$$ $p < 0.001$, and $$$$ $p < 0.0001$ significantly lower than the inflammatory effect induced by Isoptoflucon®.

Supplementary Material

Click here to download Supplementary Material: Supplementary Material.pdf